JOURNAL OF MATERIALS SCIENCE 15 (1980) 875–885

Fracture behaviour of composites based on Al_2O_3-TiC

R. P. WAHI,* B. ILSCHNER
University of Erlangen-Nürnberg, Martensstrasse 5, 8520 Erlangen, West Germany

The critical stress intensity factor and other related fracture parameters have been measured in three-point bending for pure Al_2O_3-TiC composites containing 4 to 35 volume fractions of TiC. An increase has been observed for all the parameters with increasing volume fraction of TiC. Following a study of the mode of fracture, the results are explained in terms of a linear variation of the fracture energy with the volume fraction of TiC.

1. Introduction

It has been shown [1–11] that alloying of brittle materials, in particular ceramics, to produce a two-phase structure may result in considerable improvement in their fracture toughness. In an attempt to explain these results theoretically, Lange [12] and Evans [13] have proposed models of crack propagation in two-phase brittle materials. These models envisage the pinning of the crack front by hard second-phase particles, thereby causing an improvement in strength as well as in toughness of the alloys.

Claussen and co-workers [8, 9], on the other hand, maintain that the increase in toughness in their materials is associated with microcrack formation. The various approaches for enhancing the toughness of ceramics have recently been reviewed by Evans *et al.* [14].

The fracture behaviour of coarse-grained Al_2O_3-ceramics containing particles of a second phase ($6Al_2O_3 \cdot BaO$) has been studied by the present authors [10, 11]. A good qualitative and quantitative agreement with the model of Evans was found. Measurements of the authors on very fine-grained Al_2O_3 containing precipitates of $Al_2O_3 \cdot MgO$, however, did not show any influence of the second phase [15]. For further investigation of the fracture behaviour of fine-grained ceramics, the system Al_2O_3–TiC was chosen. Fine-grained composites based on this system possess high wear resistance and as such are used in industry as tool materials for very high-speed cutting/grinding of hard materials.

2. Experimental procedure

2.1. Materials

The hot-pressed composites containing 5 to 40 wt % TiC (Table I) were supplied by Feldmühle AG, Plochingen, West Germany. All composites were produced under uniform conditions of mixing and hot pressing. For comparison, samples of hot-pressed Al_2O_3 (W304) fabricated under identical conditions were also included in the investigations.

2.2. Microstructure and fracture parameters

The porosity, P, of the composites was calculated from the measured and theoretical densities, ρ_E and ρ_T, respectively:

$$P = (\rho_T - \rho_E)/\rho_T. \quad (1)$$

Here ρ_T is the weighted average of the known theoretical densities of the two pure components [ρ_T (Al_2O_3) = 3.986 g cm^{-3} and, ρ_T (TiC) = 4.92 g cm^{-3} [16].] For the microstructural examination, the specimens were diamond polished, and the pure alumina specimens were thermally etched (30 min at 1200° C). The TiC particles could be revealed under an optical microscope in the as-polished condition. The average size of the TiC-particles, the Al_2O_3 grains and their respective distribution characteristics in the single-phase specimens were determined with the help of line intercept method [17].

The elastic modulus, E, of the composites was determined by measuring their resonance frequency, f, in a Förster Elastomat:

*Present address: Hahn-Meitner-Institute for Nuclear Research, Glienicker Straße 100, 1000 Berlin 39, West Germany.

0022–2461/80/040875–11$03.10/0

TABLE I Measured and derived parameters of Al_2O_3–TiC composites

Composites	TiC (wt%) f_w	Density (g cm^{-3})		Porosity P (%)	Volume fraction of TiC, f_v (%)	Average diameter of TiC $2\bar{R}$ (μm)	Average distance between particles $2\bar{d}$ (μm)	$\bar{R}/\bar{d}$	Critical inherent cracksize a (μm)	Elastic modulus, E (GN m^{-2})	Fracture stress, σ_B (MN m^{-2})		Critical stress intensity factor K_{IC} (MN m$^{-3/2}$)		Work of fracture, γ_F (J m^{-2})	Fracture energy, γ_I (J m^{-2})
		ρ_E	ρ_T								σ_B*	σ_B†	K_{IC}‡	K_{IC}§		
W304	0	3.966	3.986	0.50	–	–	–	–	175	393	332	305	4.10	4.55	19.4	20.4
W305	5	3.998	4.033	0.87	4.1	0.89	13.89	0.064	68	399	465	462	6.20	4.29	14.7	19.8
W306	10	4.051	4.079	0.69	8.3	0.68	5.00	0.136	56	399	536	502	6.05	4.22	14.3	18.5
W307	20	4.109	4.173	1.53	16.8	1.18	3.89	0.303	59	405	318	530	6.60	4.61	14.5	21.5
W308	30	4.211	4.266	1.29	25.8	0.77	1.48	0.522	43	410	400	635	6.16	4.69	16.1	21.3
W309	40	4.304	4.359	1.28	35.1	0.97	1.20	0.811	44	415	352	670	6.30	4.99	16.5	26.5

*Ground specimens.
†Polished specimens.
‡Machined notch.
§Natural crack.

$$E = (48l^4\pi^2\rho_E/m^4a^2)\cdot f^2. \quad (2)$$

Here l is the length of the specimen, a is a specimen dimension parallel to the vibrations in the specimen and m is a constant [18]. The accuracy of E-measurements was ± 1%. The technique also allowed the determination of Poisson's ratio, ν, whose values for these composites were found to lie between 0.23 and 0.25.

The fracture parameters, namely, the fracture strength, σ_B, the critical stress intensity factor, K_{IC}, the fracture energy γ_I and the work of fracture γ_F were measured on bar-shaped specimens of rectangular cross-section (2 mm × 4 mm × 32 mm). The specimens were fractured in three-point bending in a universal testing machine (Instron). For computing σ_B and K_{IC} from fracture load, P, and specimen geometry, the following well-known relations were used:

$$\sigma_B = 3Pl/2bw^2 \quad (3)$$

$$K_{IC} = \sigma_B\sqrt{c}\cdot Y(x) \quad (4)$$

$$\gamma_I = (K_{IC}^2/2E)(1-\nu^2). \quad (5)$$

Here l is the span of the specimen, c the notch-depth, b and w the breadth and the width of the specimen respectively, and $Y(x)$ is a correction-factor which is a function of the relative notch depth x ($x = c/w$). For specimens with $x = 0.3$, the value of $Y(x)$ given in [19] was employed, whereas for $x = 0.75$ the function suggested in [20] was used, see also [21].

Measurements of σ_B were carried out (a) on specimens whose surfaces were ground with a D30 diamond wheel, and (b) on specimens whose tension-side was diamond-polished to a finish of $R_t = 0.8$. In both cases a constant cross-head speed of 100 μm min^{-1} and a span of 30 mm were used. For the measurements of K_{IC} the following two types of cracks were employed.

(1) A sharp natural crack produced in a separate controlled fracture experiment. To obtain this, specimens with a triangular notch [22] were fractured to the base of the notch in a controlled manner [23]. The relative notch depth was maintained in all cases at 0.75 ± 0.02.

(2) A machine-cut straight edge notch (x = 0.30 ± 0.01) produced with a 0.1 mm thick diamond wheel.

In the case of specimens with natural crack, the catastrophic fracture necessary for a valid determination of K_{IC} was realized by using a shorter span (16 mm) and higher cross-head speed (500 μm min^{-1}). For specimens with machine-cut notch these parameters were the same as used for σ_B determination.

γ_F was calculated from the area under load/deflection curve obtained in a controlled fracture experiment [23].

3. Results

All the measured and derived parameters are shown in Table I. The values of the measured parameters represent an average of at least five measurements.

3.1. Microstructure

The measured densities ρ_E of the composites, shown in Table I, are plotted in Fig. 1a as a function of the volume fraction, f_v, of TiC particles. The f_v values were derived from respective weight fractions, f_w, and using theoretical densities of TiC and Al_2O_3. The variation of ρ_E with f_v is in good agreement with that of ρ_T with f_v. The calculated porosities of the composites lie between 0.5 and 1.5% (Table I). Some typical micrographs of the composites are shown in Fig. 2. The Al_2O_3 grains (Fig. 2a) as well as the particles of TiC (Fig. 2b) show a log-normal distribution (Fig. 3). The average diameter, $\bar{D}$, of the Al_2O_3 grains measured in W304 is 0.83 μm and the average diameter, $2\bar{R}$, of TiC-particles varies from 0.68 to 1.18 μm. These data show that all the composites are dense and very fine grained. The size of Al_2O_3 grains in composites (W305-W309) could not be revealed with sufficient clarity. However, since all the investigated materials were fabricated under identical conditions, it can be assumed that the grain size of Al_2O_3 in the composites is about the same as that in W304.

3.2. Fracture parameters

Variations in E, σ_B, K_{IC}, γ_I and γ_F with f_v are represented in Figs. 1 and 4. All the parameters show a rising trend with increasing f_v. In the range of f_v from 0.0 to 0.35, the relative increases in E, σ_B (polished specimens), K_{IC} (natural cracked specimens), γ_I and γ_F amount to about 5%, 56%, 38%, 46% and 22%, respectively. σ_B measured on ground specimens and K_{IC} measured on specimens with machine-cut notch, however, do not show any influence of TiC addition.

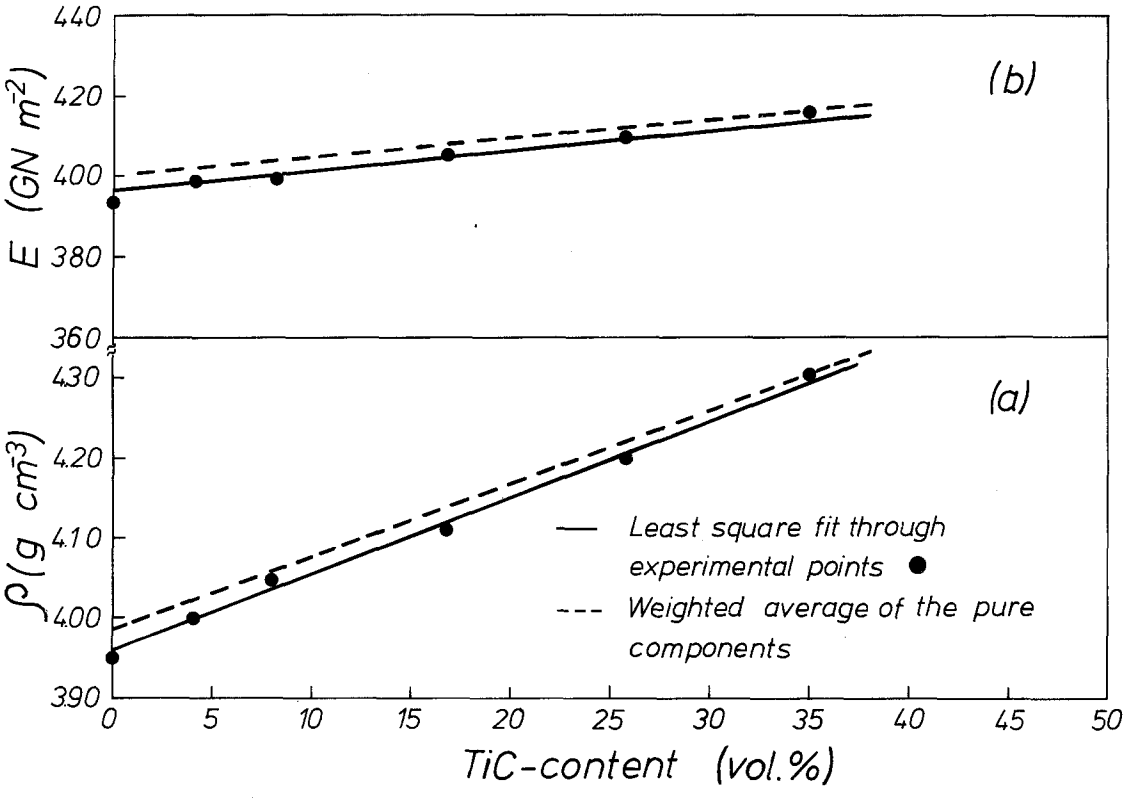

Figure 1 Variation in (a) the density, ρ, and (b) elastic modulus, E, of composites with the volume fraction, f_v, of TiC.

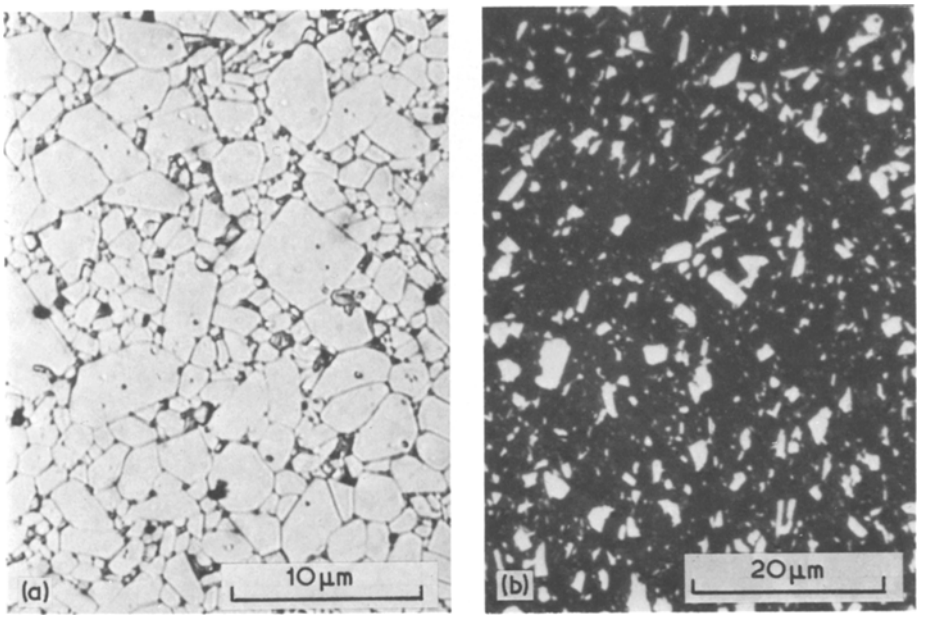

Figure 2 Microstructure of the composites. (a) Al_2O_3 grains in W304, (b) TiC particles in W307 ($f_v = 0.17$).

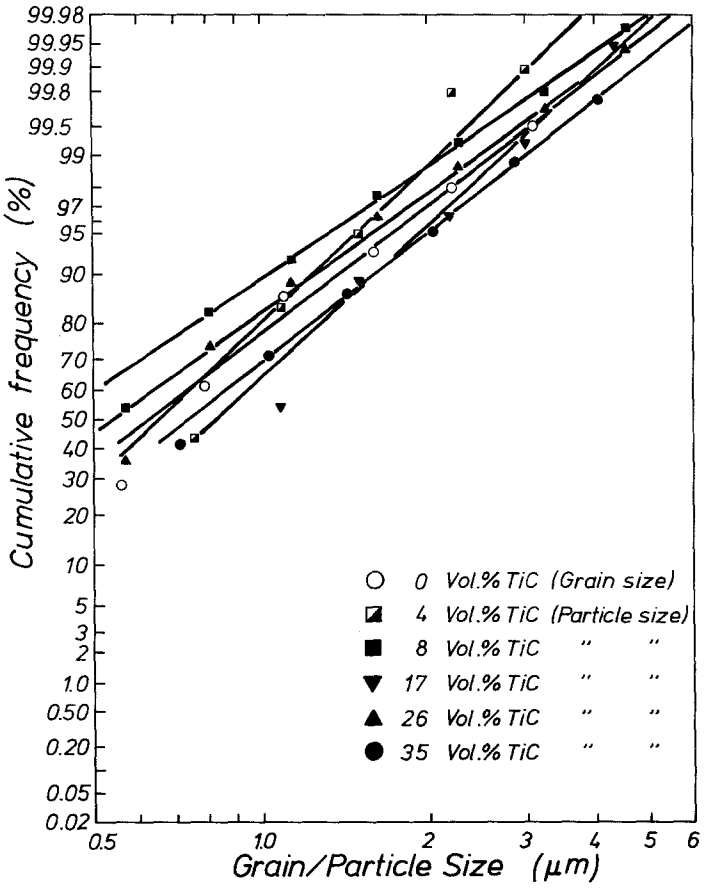

Figure 3 Distribution of grain/particle diameter.

4. Discussion

4.1. Fracture strength

The strength of brittle materials is known [24] to be markedly influenced by the nature of their surface preparation. Surface defects introduced during grinding can drastically reduce the fracture strength. In the present specimens the lowering of σ_B in all the composites caused by the grinding-induced surface defects is obviously large enough to more than compensate for the smaller increase due to TiC addition. As a result, the σ_B values do not show any variation with f_v. In contrast to this behaviour, the influence of TiC addition on σ_B is clearly brought out when the extrinsic effect due to surface damage is reduced to a minimum by polishing the tension side of the bend specimens.

The expressions for σ_B and K_{IC}, according to Griffith and Irwin, respectively, are:

$$\sigma_B = \frac{1}{Y(x)}\left(\frac{2E\gamma_I}{c\cdot(1-\nu^2)}\right)^{1/2} \quad (6)$$

$$K_{IC} = \left(\frac{2E\gamma_I}{1-\nu^2}\right)^{1/2} \quad (7)$$

or

$$\sigma_B = \frac{K_{IC}}{y(x)\cdot\sqrt{c}}. \quad (8)$$

According to Equation 8, the observed variation in fracture stress with the volume fraction, f_v, of TiC must be due to variations in K_{IC} and flaw-size, c, with f_v. Since the total fractional increase in σ_B (56%) is larger than the total fractional increase in K_{IC} (38%), a part of the increase in fracture stress must be done to corresponding decrease in flaw size with f_v. A rough measure of the notch depth, c, is given by $(K_{IC}^2/\sigma_B^2)\cdot(\pi/4)$. Fig. 5 shows a plot of the computed values of $\sqrt{c}$ as a function of f_v. As expected from Figs. 4a to c, the value of $\sqrt{c}$ falls with increasing f_v. Dispersion of TiC particles appear to restrict the size of inherent flaws in the composites and thereby further contributes to their strength.

4.2. Stress intensity factor

For valid K_{IC} measurements on ceramics using notched specimens, it is essential to keep the notch-root radius (= 1/2 notch width) smaller than a critical value which is a material parameter

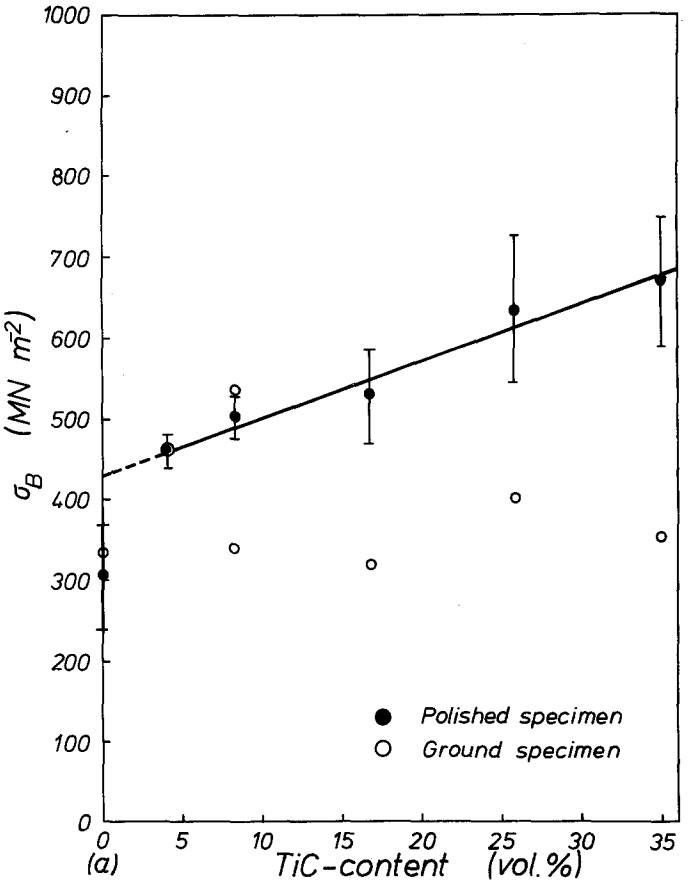

Figure 4 Variation in (a) fracture stress, σ_B, (b) critical stress intensity factor, K_{IC}, (c) fracture energy, γ_I, and work of fracture, γ_F, with f_v.

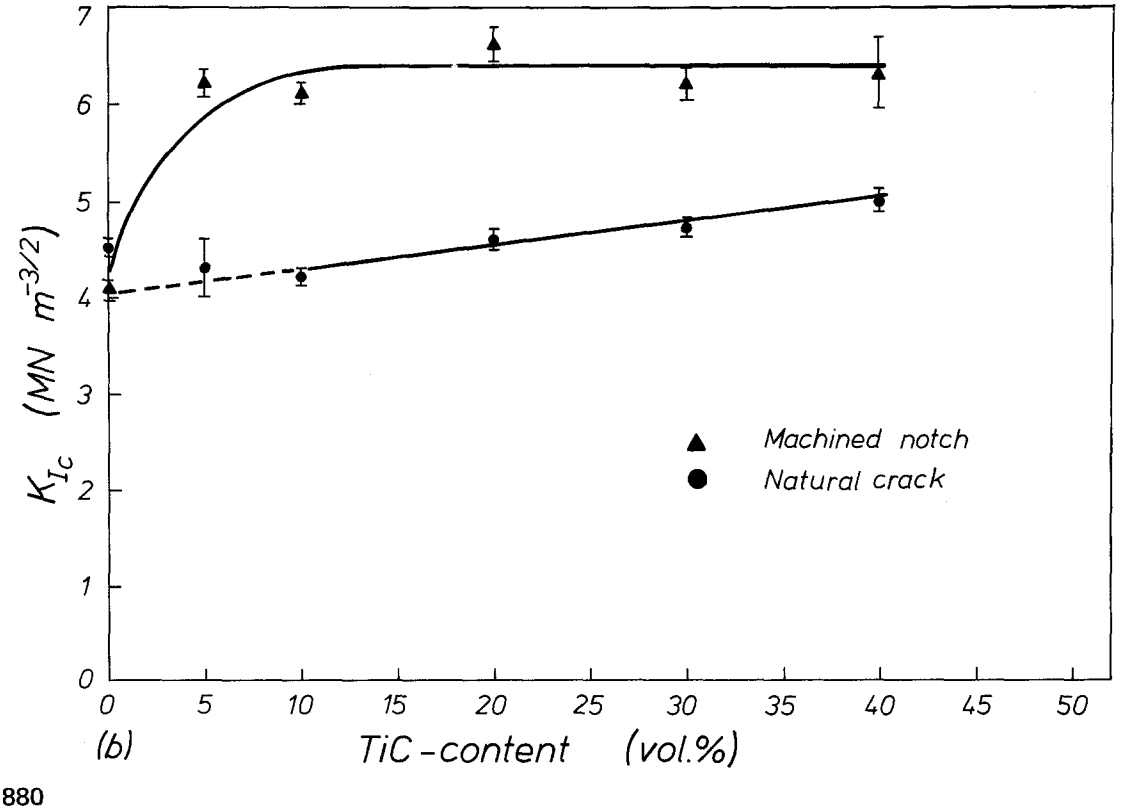

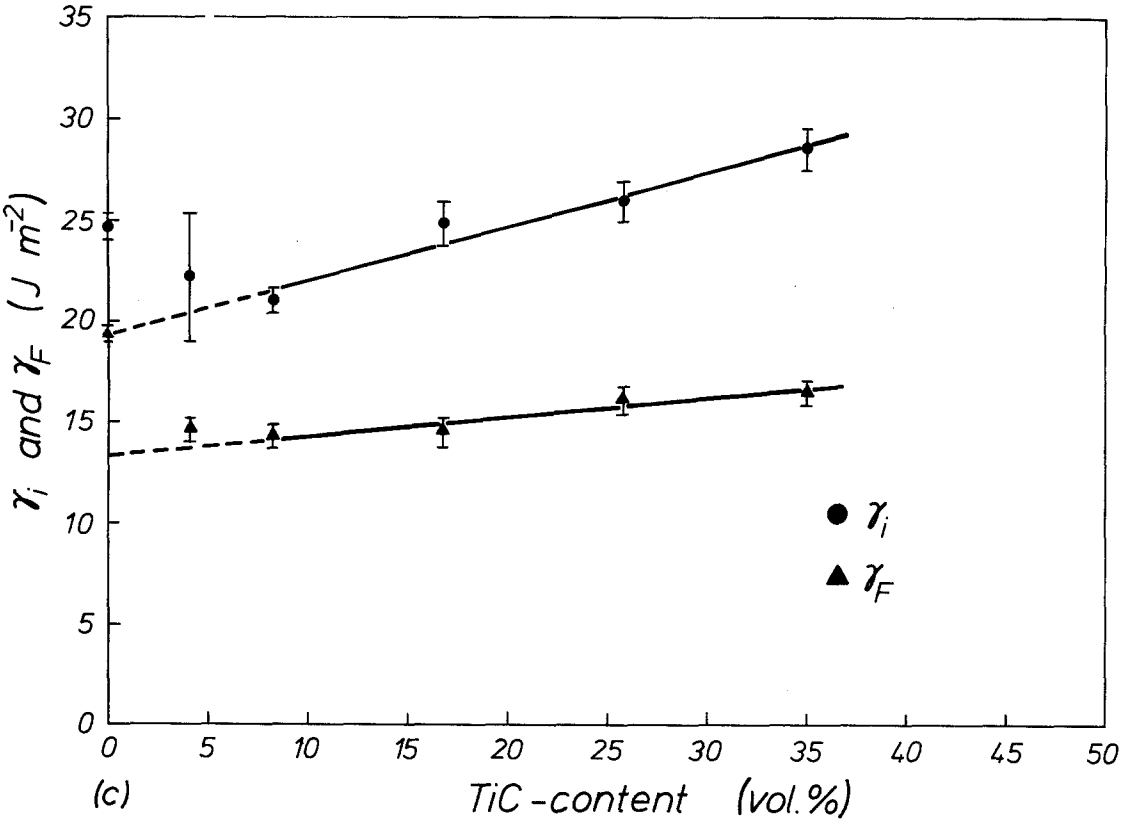

Figure 4 Continued

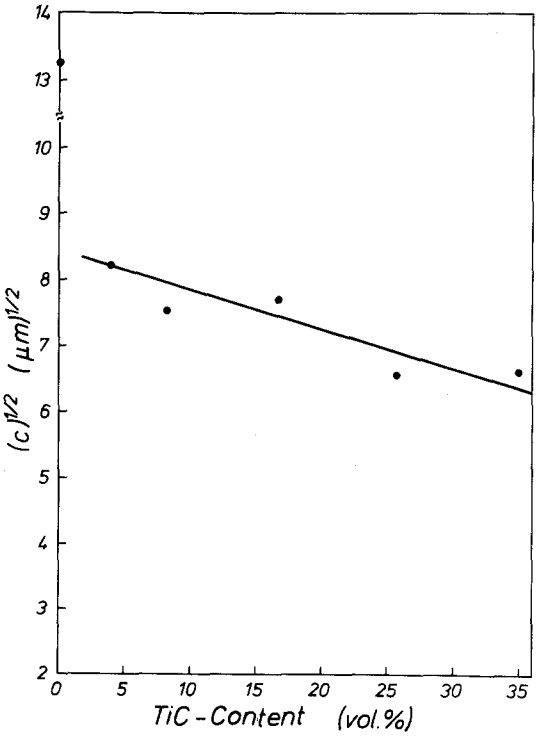

Figure 5 Variation in the inherent crack size c with f_v.

[25, 26]. Use of notches of larger width results in an over-estimation of K_{IC} which increases with notch width [26]. In case of fine-grained Al_2O_3 it has been shown [25, 27] that a notch width of $\leqslant 0.1$ mm is necessary for valid K_{IC} measurement. Our results on hot-pressed Al_2O_3 (W304) using a machined notch of 0.1 mm width confirm this. The measured value of 4.1 MN m$^{-3/2}$ is in good agreement with K_{IC} value for Al_2O_3 of comparable porosity measured in [25], using double cantilever beam specimens. In case of the composites, however, the critical notch root-radius appears to be smaller than 0.05 mm employed in the present investigations. The apparent high values of K_{IC} ($\simeq 6$ MN m$^{-3/2}$) measured in all the composites using notched specimens therefore do not allow the influence of TiC additions to be seen (Fig. 4b). However, when the effect of notch root-radius was eliminated by using specimens with sharp natural cracks, a small but distinct influence of TiC addition on K_{IC} could be detected.

In terms of the model of Evans the expected increase in K_{IC} as a function of the parameter $\bar{R}/\bar{d}$ can be computed using Equations 18 and 19 of Evans [13] and taking the K_{IC} value of Al_2O_3

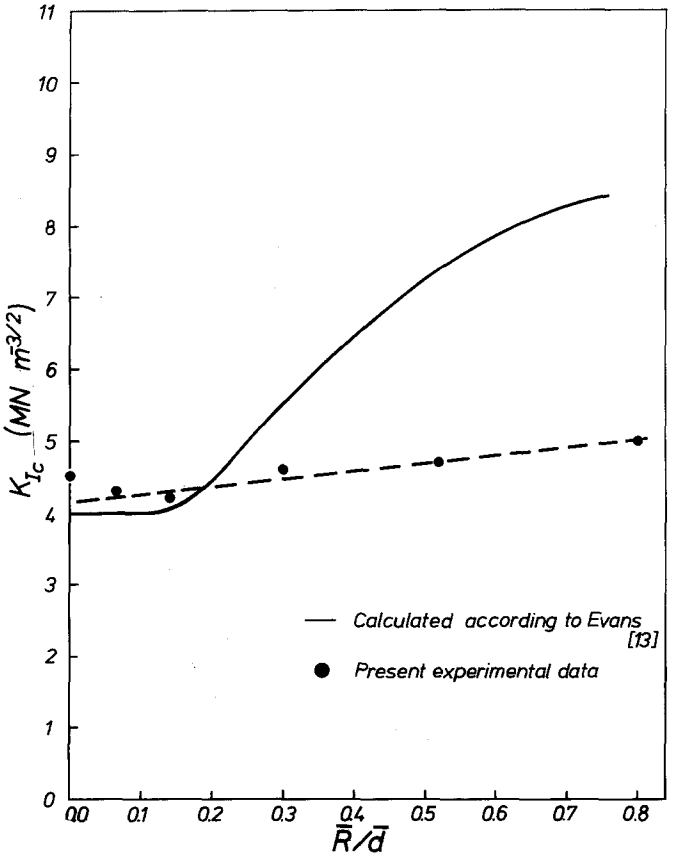

Figure 6 K_{IC} as a function of $\bar{R}/\bar{d}$.

to be 4 MN m$^{-3/2}$. The computed values of K_{IC} corrected for crack interaction at the back of the particles are shown as a function of $\bar{R}/\bar{d}$ in Fig. 6. For comparison, the measured values of K_{IC} are also included in the same diagram. The average spacing $2\bar{d}$ between the particles in the present composites was calculated from the respective f_v and $\bar{R}$ values according to Fullman [28]. It is evident that the experimentally determined rise in K_{IC} as a function of $\bar{R}/\bar{d}$ is much smaller than the increase expected in terms of the theoretical model. Moreover, the fracture surface of the composites does not show the characteristic feature expected on the basis of the crack-pinning model. As a consequence of the bowing of crack front between the particles of second phase and a reunion of the two branches of the crack front on the back side of the particles, wedge-shaped cleavage steps are expected to form on this side of the particles. Such steps have been observed by Lange [1] and by Wahi *et al.* in Al_2O_3–BaO alloys [11]. On the fracture surface of the present composites, these steps could not be detected. Instead, an examination of the fracture surface showed that TiC particles mostly had a transcrystalline fracture. This observation is in agreement with the result of Chermant *et al.* [29] who have reported a predominantly transcrystalline fracture in pure TiC. Some typical fractographs are shown in Fig. 7. TiC particles with fine cleavage steps running through the grains are clearly to be seen. The particles could be identified by means of EDAX analysis of the fracture surface.

If the crack front cuts through the particles instead of bypassing them, the average fracture energy, γ_I, of the composites should, to a first approximation, lie between the fracture energies of Al_2O_3 and TiC and vary linearly with the fraction of the total fracture surface, f_s, occupied by TiC. Now turning to Equation 7, E has been found experimentally to vary linearly with f_v (Fig. 1b). If γ_I were also to be a linear function of f_v (according to [25] $f_s = f_v$), the expression for K_{IC}^2 from Equation 7 could be written as follows:

$$K_{IC}^2 = 2\{(E_2 - E_1)\cdot f_v + E_1\} \times \{(\gamma_2 - \gamma_1)\cdot f_v + \gamma_1\} \quad (9)$$

or

$$K_{IC}^2 = 2\{(\Delta E\cdot\gamma_1 + \Delta\gamma\cdot E_1) \times f_v + E_1\cdot\gamma_1 + \Delta E\cdot\Delta\gamma\cdot f_v^2\}. \quad (10)$$

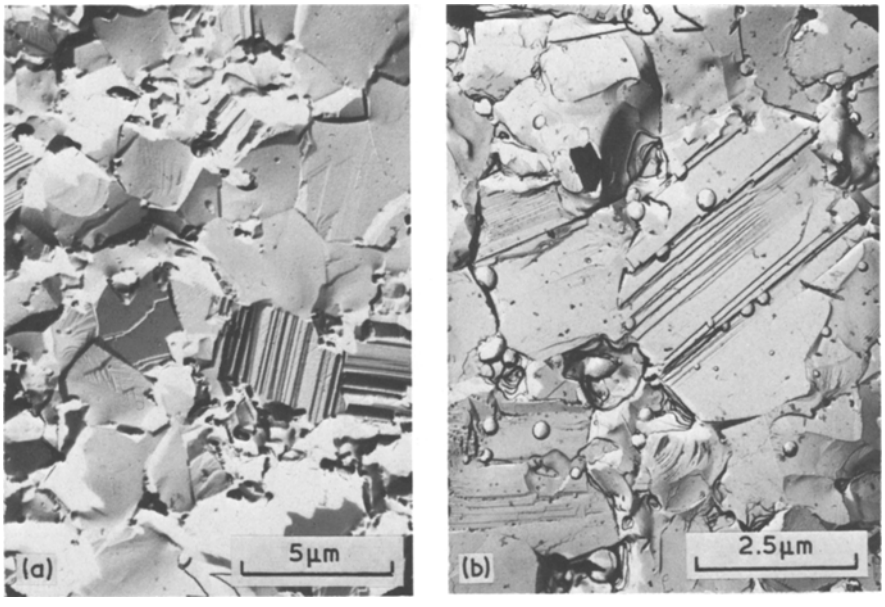

Figure 7 Some typical fractographs. (a) W307 ($f_v = 0.17$), (b) W309 ($f_v = 0.35$).

Neglecting the term $\Delta E \cdot \Delta\gamma \cdot f_v^2$ which is small compared to the rest of the terms, K_{IC}^2 can be approximately written as a linear function of f_v:

$$K_{IC}^2 = 2\{(\Delta E \cdot \gamma_1 + \Delta\gamma \cdot E_1) \cdot f_v + E_1 \cdot \gamma_1\}. \quad (11)$$

Here ΔE and $\Delta\gamma$ are the differences between the E-values and γ_I values of Al_2O_3 and TiC, respectively, and E_1 and γ_1 are the elastic modulus and fracture energy, respectively, of Al_2O_3.

Fig. 8 shows a plot of K_{IC}^2 as a function of f_v. The experimental points lie fairly close to the straight line drawn on the basis of least squares fit. An extrapolation of the straight line to 100% TiC leads to a K_{IC}^2 value of 40.10 $MN^2\,m^{-3}$ which corresponds to a K_{IC} of 6.33 $MN\,m^{-3/2}$ for pure TiC.

Mai [30] has measured K_{IC} of dense TiC (employing specimens with natural crack) to be 7.5 $MN\,m^{-3/2}$. In view of the simplifying assumptions made in arriving our Equations 11 and the large extrapolation of the experimental values involved, a difference of about 15% between the two values of K_{IC} appears to be small. Two other independent measurements of K_{IC} on TiC, on the other hand, report values of 3.8 $MN\,m^{-3/2}$ [29] and 3.9 $MN\,m^{-3/2}$ [31] which do not fit in the above model. The density of TiC in [29], however, appears to be smaller than that of our materials. Moreover, the nature of the crack employed in [29] is not clear. Both these factors can considerably influence the K_{IC} value. The measurements in [31] are made on dense TiC using natural crack, as in the present work.

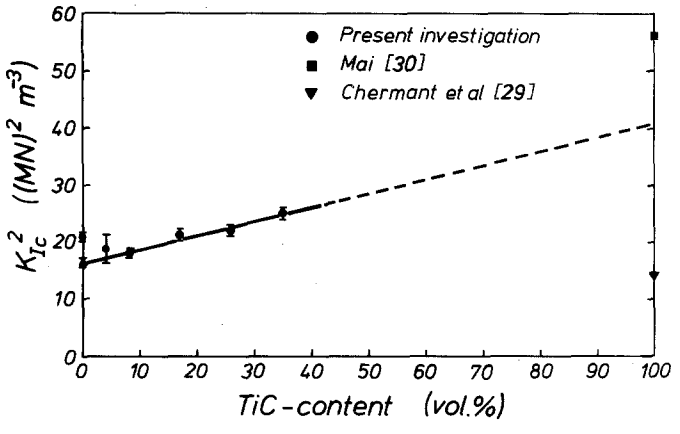

Figure 8 Variation in K_{IC}^2 as a function of f_v.

Let us now consider the possible influence of microcracks on the fracture behaviour. It has been shown [32] that microcracks may form in two-phase brittle materials as a result of different coefficients of linear thermal expansion, α, of the matrix and the second phase. The cracks would form provided the second-phase particles are larger than a critical size, R_c, which is inversely proportional to the square of the difference $\Delta\alpha$ in the two α values. In ceramics such as Al_2O_3 containing ZrO_2 where considerable improvement in fracture toughness has been achieved through microcracks [8, 9], the effective value of $\Delta\alpha$ is quite large ($2.8 \times 10^{-5}\,^{\circ}C^{-1}$). This means that even very small particles of ZrO_2 ($\simeq 1\,\mu m$) are able to initiate cracks. The toughness can be improved therefore, through uniformly distributed fine microcracks. In the present composites, however, $\Delta\alpha$ amounts only to $5.6 \times 10^{-6}\,^{\circ}C^{-1}$ [$\alpha(Al_2O_3) = 8 \times 10^{-6}\,^{\circ}C^{-1}$ and $\alpha(TiC) = 2.4 \times 10^{-6}\,^{\circ}C^{-1}$ [16]]. The value of R_c for TiC particles can be calculated using the Equation 12 in [32]. Assuming the parameter $H(\mu p)$ in the above equation to be unity and substituting values for the other parameters from the present investigation (E for TiC from [31] and the α-values from [16]) one obtains $R_c \simeq 4\,\mu m$. Thus it appears that microcracks may not play an important role in the present composites, since the average size of the particles is much smaller (0.34 to 0.59 μm). However, unless $H(\mu_0)$ is correctly known (it is likely to be smaller than unity) the possibility of a microcrack influence cannot be completely ruled out.

5. Conclusions

The fracture behaviour of Al_2O_3–TiC ceramics containing a wide range of volume fraction of TiC has been investigated. The study of the dependence of fracture parameters as a function of the volume fraction, f_v, of TiC has lead to the following conclusions:

(1) addition of TiC results in a small but distinct increase in K_{IC},

(2) the observed increase in K_{IC}, within the range of investigated composites, shows a good agreement with the proposed model of linear dependence of K_{IC}^2 on f_v,

(3) use of a machined notch of 0.1 mm thickness in three-point bent specimens of the composites results in an overestimating of K_{IC},

(4) the size of the inherent flaws in the composites appears to depend on f_v – decreasing with increasing f_v. The fracture stress, therefore, shows a stronger dependence on f_v than shown by K_{IC}.

Acknowledgements

One of the authors (R. P. Wahi) gratefully acknowledges the financial support provided by the German Association for Industrial Research (AIF) for the pursuit of this investigation under project no. AIF 3555. The authors also wish to thank Dr W. Grellner and Mr H. Hupke for contributing measurements of elastic modulus, and for assistance in experimental work, respectively. Finally thanks are due to Dr H. Kleinlein and Mr M. Wünschmann for valuable discussions and comments.

References

1. F. F. LANGE and K. C. RADFORD, *J. Mater. Sci.* 6 (1971) 1197.
2. F. F. LANGE, *J. Amer. Ceram. Soc.* 54 (1971) 614.
3. *Idem ibid* 56 (1973) 445.
4. G. K. BANSAL and A. H. HEUER, "Fracture Mechanics of Ceramics", Vol. 2, edited by R. C. Bradt, D. P. H. Hasselman and F. F. Lange (Plenum Press, New York, 1974) p. 677.
5. M. I. MENDELSON and M. E. FINE, *J. Amer. Ceram. Soc.* 52, (1974) 154.
6. C. AHLQUIST, *Acta Met.* 23 (1975) 239.
7. G. K. BANSAL and A. H. HEUER, *J. Amer. Ceram. Soc.* 58 (1975) 235.
8. N. CLAUSSEN, *ibid* 59 (1976) 49.
9. N. CLAUSSEN and J. STEEB, *ibid* 59 (1976) 457.
10. R. P. WAHI and H. HÜBNER, *Ber. Deut. Keram. Ges.* 53 (1976) 423.
11. R. P. WAHI, H. HÜBNER and B. ILSCHNER, Proceedings of the 2nd International Conference on Mechanical Behaviour of Materials, Boston, USA (1976).
12. F. F. LANGE, *Phil. Mag.* 22 (1970) 983.
13. A. G. EVANS, *ibid* 26 (1972) 1327.
14. A. G. EVANS, A. H. HEUER and D. L. PORTER, Proceedings of the 4th International Conference on Fracture, Waterloo, Canada (1977).
15. R. P. WAHI and B. ILSCHNER, unpublished work.
16. "Engineering Properties of Selected Ceramic Materials" (American Ceramic Society Ohio, USA, 1966).
17. H. E. EXNER, *Pract. Metallogr.* 3 (1966) 334.
18. E. GOENS, *Ann. Phys.* B11 (1931) 649.
19. W. F. BROWN and J. E. SRAWLEY, Plane Strain Fracture Toughness Testing of High-Strength Metallic Materials, ASTM Special Technical Publication No. 410, Philadelphia, USA (1966).
20. W. K. WILSON, *Eng. Fract. Mech.* 2 (1970) 169.
21. H. HÜBNER and H. SCHUHBAUER, *ibid* 9 (1977) 403.

22. H. G. TATTERSALL and G. TAPPIN, *J. Mater. Sci.* **1** (1966) 296.
23. U. ENGEL and H. HÜBNER, *ibid* **13** (1978) 2003.
24. B. G. KOEPKE and R. S. STÖKES, *ibid* 7 (1970) 983.
25. L. A. SIMPSON, *J. Amer. Ceram. Soc.* 57 (1974) 151.
26. F. E. BURESCH, Deutscher Verband für Materialprüfung, Arbeitskreis Bruchvorgänge, Band 8, Köln, West Germany (1976).
27. R. L. BERTOLOTTI, *J. Amer. Ceram. Soc.* 56 (1973) 107.
28. R. L. FULLMAN, *J. Metals* 5 (1953) 447.
29. J. L. CHERMANT, A. DESCHANVERS and F. OSTERSTOCK, Proceedings of the Symposium on Fracture Mechanics of Ceramics, Pennsylvania State University, Pennsylvania, USA (1977).
30. Y. W. MAI, *J. Amer. Ceram. Soc.* 59 (1976) 491.
31. M. WÜNSCHMANN, Diplom-Thesis, University of Erlangen-Nürnberg, Erlangen, West Germany (1978).
32. F. F. LANGE, "Fracture Mechanics of Ceramics", Vol. 2 edited by R. C. Bradt, D. P. H. Hasselman and F. F. Lange (Plenum Press, New York, 1974) p. 599.

Received 5 July and accepted 24 July 1979.